LOCAL BOND STRESS-SLIP RELATIONSHIPS OF DEFORMED BARS UNDER GENERALIZED EXCITATIONS

By R. Eligehausen[I], E.P. Popov[II], and V.V. Bertéro[II]

SUMMARY

The local bond stress-slip relationships of deformed bars embedded in confined concrete under monotonic and cyclic loading for various bond conditions were investigated in an extensive experimental study. The results were used to deduce an analytical model of the bond behavior under random excitations. By evaluating experimental results of long anchorages, the model was extended to cover the bond conditions found in joints of R/C frames under severe seismic excitations. The model was successfully used to predict the behavior of deformed bars anchored at interior joints and subjected to various loading histories.

1. INTRODUCTION

The behavior of bond between deformed bars and concrete under severe seismic excitations, which highly influences the response of reinforced concrete structures /1,2/, is not yet well known /3/. Therefore extensive experimental and analytical studies were carried out to obtain local bond stress-slip relationships under general excitations.

2. EXPERIMENTAL PROGRAM

The test specimens (Fig. 1) represented the confined region of a beam-column joint. Only a short length ($5d_b$) of a grade 60 deformed bar was embedded in concrete. Because cracking might influence the bond stress-slip behavior, the resistance against splitting was simulated as closely as possible to that which might exist in a real structure. Therefore a thin plastic sheet was placed in the plane of the longitudinal axis of the bar (Fig. 1) which limited the concrete splitting area to the desired value, depending on the assumed bar spacing.

The test specimen was installed in a specially designed testing frame (Fig. 2) and was loaded by a hydraulic servo controlled universal testing machine. The tests were run under displacement control by subjecting the threaded loading end of the bar to the required force needed to induce the desired slip, which was measured at the unloaded bar end and was usually controlled at a rate of 1.7 mm/min.

In the main test series # 8 (25,4 mm) bars were embedded in a concrete with $f_c' = 30$ N/mm², the assumed spacing was 4 d_b and the secondary reinforcement consisted of # 4 (12,7 mm) bars. The influence of various slip histories on the bond stress-slip behavior was examined. In other test series the influence of the following parameters on the bond behavior under monotonic and cyclic loading was studied: Confining reinforcement, bar diameter,

---

I Senior Research Engineer, University of Stuttgart, West Germany, formerly Visiting Scholar at the University of California, Berkeley, USA

II Professor, University of California, Berkeley, USA

concrete strength, bar spacing, transverse pressure and rate of slip increase. Usually 2 or 3 identical tests were carried out. Altogether some 120 specimens were tested.

3. EXPERIMENTAL RESULTS

3.1 Monotonic Loading

Typical test results are shown in Fig. 3 and summarized below:

(a) The bond stress-slip relationship for monotonic loading in tension was almost identical to that in compression. This could be expected /5/ since the specimens were cast with the bars in a horizontal position.

(b) The descending branch of the bond stress-slip curve levelled off at a slip approximately equal to the clear distance between protruding lugs of the bar. This can be seen from Fig. 3b. The clear distance between lugs was 7,5 mm, 11,0 mm and 10,5 mm for bars with $d_b \sim$ 19,25 and 32 mm respectively.

(c) Specimens without secondary reinforcement failed by splitting of the concrete in the plane of the tested bar. Splitting cracks were also observed in the other tests, however, their growth was controlled by the vertical bars. Failure was caused by pull-out well below yield stress. Restraining reinforcement increased the bond strength and significantly improved the overall behavior (Fig. 3c).

(d) The bond resistance at given slip values was approximately proportional to $\sqrt{f_c'}$.

(e) The bond behavior was slightly improved by increasing the clear distance between bars (Fig. 3d).

(f) With increasing pressure, applied transversely to the plane of splitting, maximum bond resistance and ultimate frictional bond resistance were increased (Fig. 3e).

(g) The bond stress-slip relationship was influenced by the rate of slip increase (Fig. 3d), however, slightly less than predicted in /3/.

3.2 Cyclic Loading

Typical results of the main test series are shown in Fig. 4 and summarized below:

(a) When the bar was loaded monotonically to an arbitrary slip value, then cycled up to 10 times between this slip value and a slip value corresponding to a load equal to zero and after that loaded to increasing slip values, the monotonic envelope was, for all practical purposes, reached again and followed thereafter.

(b) If the peak bond stress in tension and compression during cycling did not exceed 70-80 percent of the monotonic τ_{max}, the ensuing bond stress-slip relationship, at slip values larger than the one at which the specimen was cycled, was not significantly affected by up to 10 cycles (Fig. 4a).

(c) Loading to slip values inducing a τ larger than 80 percent of the monotonically obtained τ_{max} in either direction led to a degradation in the bond stress-slip behavior in the reversed direction (Figs. 4b and 4c). The bond resistance at slip values larger than the peak value during previous cycles increasingly deteriorated with increasing peak slip s_{max}, increasing difference between the peak slip values between which the bar was cyclically loaded, and increasing number of cycles (Fig. 4b and 4c). The largest deterioration was observed for full reversals of slip.

(d) The frictional bond resistance, τ_f, during cycling was dependent upon the value of the peak slip s_{max}. With repeated cycles τ_f deteriorated rapidly.

(e) The behavior of bond during cycling loading was not significantly effected by the various parameters investigated, if the deterioration of bond resistance was related to the pertinent monotonic envelope.

(f) The observed behavior is not well described by existing analytical models /3,6,7/.

A detailed explanation of the observed behavior is given in /4/.

4. ANALYTICAL LOCAL BOND STRESS-SLIP MODEL

The test results were used to deduce an analytical model for the local bond stress-slip relationship valid for confined concrete under generalized excitations (Fig. 5). It was published in /7/ and extended in /4/ to cover different bond conditions and the variation of bond behavior along the embedment length.

4.1 Confined concrete

The main characteristics of the bond model are described below by following a typical cycle (Fig. 5):

When loading the first time, the assumed bond stress-slip relationship follows the "monotonic envelope" valid for monotonically increasing slip (paths OABCD or $OA_1B_1C_1D_1$). Imposing a slip reversal at an arbitrary slip value, a stiff "unloading branch" and the "friction branch" with $\tau = \tau_f$ are followed successively up to the intersection with the curve OA_1' (path EFGHI). Then the "reduced envelope" (curve $OA_1'B_1'C_1'D_1'$) which is similar to the virgin monotonic curve but with reduced values of τ is followed (path $IA_1'J$). When reversing the slip again at J, unloading branch, frictional branch and "reloading branch" (same stiffness as the unloading branch) are followed successively up to the intersection with the reduced envelope O A'B'C'D' (path JLNE'), which is followed thereafter (path E'B'C'). If instead of increasing the slip beyond point N more cycles between the slip values corresponding to the points N and K are imposed, the bond stress-slip relationship is like that of a rigid plastic model, but with decreasing frictional bond resistance as the number of cycles increases. In the following details about the different branches are given.

(a) Monotonic Envelope

The monotonic envelope consists of an initial non-linear relationship $\tau = \tau_1 (s/s_1)^{\alpha}$ valid for $s \leq s_1$, followed by a plateau $\tau = \tau_1$ for $s_1 \leq s \leq s_2$.

For $s \geq s_2$, τ decreases linearly to the value of the ultimate frictional bond resistance τ_3 at a slip value of s_3. This value s_3 is assumed to be equal to the clear distance between the lugs of the deformed bars.

With the values s_1 = 1,0 mm, s_2 = 3,0 mm, s_3 = 11,0 mm, τ_1 = 13,5 N/mm², τ_3 = 5,0 N/mm² and $\alpha = 0{,}4$ the analytically obtained bond stress-slip relationship agrees well with the average curve obtained in the main test series. For bond conditions different from those in these tests, the information given in section 3.1 can be used to modify the characteristic values describing the monotonic envelope. For more detailed information see /4/.

(b) Reduced envelopes

Reduced envelopes are obtained from the monotonic envelope by reducing the characteristic bond stresses τ_1 and τ_3 through a "damage parameter" d. For no damage, d = 0, the reloading branch reaches the monotonic envelope. For full damage, d = 1, bond is completely destroyed ($\tau = 0$).

It is assumed that deterioration of bond stiffness and bond strength during cyclic loading is caused by damage of the concrete between lugs which in turn is a function of the dissipated energy. Fig. 6 illustrates the correlation between the measured damage factor d, for tests with full reversal of slip, as a function of the computed dimensionless dissipated energy factor E/E_o. The proposed function for d is shown as well. In the computation of E only 50 % of the energy dissipated by friction was taken into account, because the other part appeared to be used to overcome the frictional resistance causing damage. The normalizing energy E_o corresponds to the absorbed under monotonically increasing slip up to the value s_3. In this way, the influence of various bond conditions can easily be taken into account.

The assumption, that damage is related to the dissipated energy, is acceptable in the range of low cycle fatigue and allows an easy generalization of the bond model to random cyclic.

(c) Frictional Resistance

The frictional bond resistance after first unlading ($\bar{\tau}_f$ in Fig. 5) depends upon the peak value of slip, s_{max}, and is related to the value of the ultimate frictional bond resistance of the corresponding reduced envelope ($\bar{\tau}_3$ in Fig. 5). The relationship found in the tests is shown in Fig. 7. The analytical function oabc is used only for the calculation of the frictional resistance for the first slip reversal. For subsequent cycles τ_f (e.g., τ_f^+ in Fig. 5) is deduced from this initial value by reducing it through an additional damage factor d_f, which depends on the energy dissipated by friction alone. Fig. 8 illustrates the correlation between the measured damage factor d_f as a function of the computed dimensionless dissipated energy E_f/E_{of}. The normalizing energy E_{of} is equal to the product $s_3 \cdot \tau_3$ and thus related to the monotonic envelope. If tests with small values E_f/E_{of} are neglected, the agreement between analytical and experimental results seems acceptable.

(d) Unloading and Reloading Branch

The slope K of the unloading and reloading branch is assumed as constant with K = 180 N/mm², valid for f_c' = 30 N/mm².

4.2 Unconfined Concrete

The bond conditions vary along the bar embedment length. For an interior joint, three different regions have been identified /7/ (Fig. 9). Under monotonic loading, the bond behavior at the tensioned bar end in the unconfined regions 1 and 2 of the joint is rather inferior compared to the confined concrete because of the early formation of a concrete cone. The opposite is true at the compressed bar end because of external and internal pressure on the bar. Of course, there is a gradual variation in bond behavior when proceeding from the unconfined region 1 or 2 to the confined one (Fig. 10).

Based on the results given in /7,9/ the following values describing the monotonic envelope in the unconfined regions are proposed for 25 mm bars and a concrete with $f_c' = 30$ N/mm². Tensioned bar end: $s_1 = s_2 = 0{,}3$ mm, $s_3 = 1{,}0$ mm, $\tau_1 = 5$ N/mm², $\tau_3 = 0$, $\alpha = 0{,}4$; compressed bar end: s_1, s_2, s_3, α as in confined region, $\tau_1 = 20$ N/mm², $\tau_3 = 7{,}5$ N/mm². The length of the unconfined regions is taken as $2\,d_b$. The middle part of the joint ($a \leq x \leq l_e - a$, with $a = 0{,}25\,l_e \leq 5\,d_b$ and l_e = embedment length) is considered as confined and a linear variation of the bond behavior from the unconfined region to the confined one is assumed.

During cycling loading more damage is induced at the tensiond bar end in the unconfined region compared to the confined one because the concrete is prone to early cone formation. It is reasonable to assume, that, once a cone has formed, not much bond resistance is left. On the contrary the mechanism of bond damage at the compressed bar end is not much different from those in the confined region. To take this behavior into account, the normalizing cyclic parameters (E_o, E_{of} and s_3) are related to the monotonic envelope of the compressed bar end and the energy dissipated at the tensioned bar end is multiplied with an amplification factor.

Due to the lack of proper experimental information the above proposals are rather crude and they should be checked by additional tests. However, when using them, a satisfactory agreement between analytically obtained and experimentally observed behavior of long anchorages was found /10/.

5. COMPARISON OF ANALYTICAL PREDICTIONS OF LOCAL BOND STRESS-SLIP RELATIONSHIPS WITH EXPERIMENTAL RESULTS

The local bond stress-slip relationships, obtained using the model described in section 4.1, are compared in Fig. 4 with the experimental results obtained in some of the Berkeley tests. As can be seen, except for the reloading curves near the values of the peak slip between which the specimen was cycled, the agreement is quite good. In general the model was successful in reproducing most of the experimental results for the various bond conditions.

6. CONCLUSIONS

From the results obtained in this study the following main observations can be made:

(1) During cycling loading the degradation of bond strength and bond stiffness depends primarily on the maximum value of peak slip in either direction reached previously. Other significant parameters are the number of cycles and

the difference between the peak values of the slip between which the bar is cyclically loaded.

(2) Cycling up to 10 times between slip values corresponding to bond stresses smaller than approximately 80 percent of the maximum bond resistance, τ_{max}, attained under monotonically increasing slip, reduces moderately the bond resistance at the peak slip value as the number of cycles increase, but does not siginificantly effect the bond stress-slip behavior at larger slip values.

(3) Cycling between slip limits larger than that corresponding to a bond stress of 80 percent of τ_{max} produces a pronounced deterioration of the bond stiffness at slip values smaller than the peak slip value and has a distinct effect on the bond stress-slip behavior at larger slip values.

(4) The behavior of bond during cyclic loading is not significantly effected by the various parameters investigated, if the deterioration of bond resistance is related to the pertinent monotonic envelope.

(5) The proposed model for the local bond stress-slip law is very simple compared with the real behavior but provides a satisfactory agreement with experimental results under various slip histories and various bond conditions.

ACKNOWLEDGEMENTS

The work reported herein was sponsored by the National Science Foundation, under grant PFR79-08984 with the University of California, Berkeley. The support of Dr. Eligehausen by the Deutsche Forschungsgemeinschaft is gratefully acknowledged.

REFERENCES

/ 1/ Popov, E.P., "Mechanical Characteristics and Bond of Reinforcing Steel under Seismic Conditions", Proceedings, Workshop on Earthquake-Resistant Reinforced Concrete Building Construction, University of California, Berkeley, July 11-15, Vol. II, pp. 658-682

/ 2/ Ma, S.Y., Bertero, V.V., and Popov, E.P., "Experimental and Analytical Studies on the Hysteretic Behavior of Reinforced Concrete Rectangular and T-Beams", Report No. EERC 76-2, Earthquake Engineering Research Center, University of California, Berkeley, 1976

/ 3/ Tassios, T.P., "Properties of Bond between Concrete and Steel under Load Cycles Idealizing Seismic Actions", Bulletin d'Information No.131 of the Commité Euro-International du Béton, Paris, April 1979

/ 4/ Eligehausen, R., Bertero, V.V. and Popov, E.P., "Local Bond Stress-Slip Relationships of Deformed Bars under General Excitations, Tests and Analytical Model", UCB-report 1982, University of California, Berkeley, to be published

/ 5/ Rehm, G., "Über die Grundlagen des Verbundes zwischen Stahl und Beton", Schriftenreihe des Deutschen Ausschusses für Stahlbeton, Berlin, 1961

/ 6/ Morita, S. and Kaku, T., "Local Bond Stress-Slip Relationship and Repeated Loading", IABSE Symposium, Resistance and Ultimate Deformability of Structures Acted on by Well-Defined Repeated Loads, Lisbon,1973

/ 7/ Viwathanatepa, S., Popov, E.P., and Bertero, V.V., "Effects of Generalized Loadings on Bond of Reinforcing Bars Embedded in Confined Concrete Blocks", Report No. EERC 79-22, Earthquake Engineering Research Center, University of California, Berkeley, 1979

/ 8/ Ciampi, V., Eligehausen, R., Bertero, V.V. and Popov, E.P., "Analytical Model for Deformed Bar Bond under Generalized Excitations", Proceedings, IABSE Colloquium an "Advanced Mechanics in Reinforced Concrete", Delft, June 1981

/ 9/ Cowell, A., "An Investigation of Local Bond Slip under Variation of Specimen Parameters", CE 299 Report, University of California, Berkeley, June 1981

/10/ Ciampi, V., Eligehausen, R., Bertero, V. and Popov, E., "Hysteretic Behavior of Deformed Reinforcing Bars under Seismic Excitations, Paper to be presented at the Seventh European Conference on Earthquake Engineering, Athens, Sept. 1982

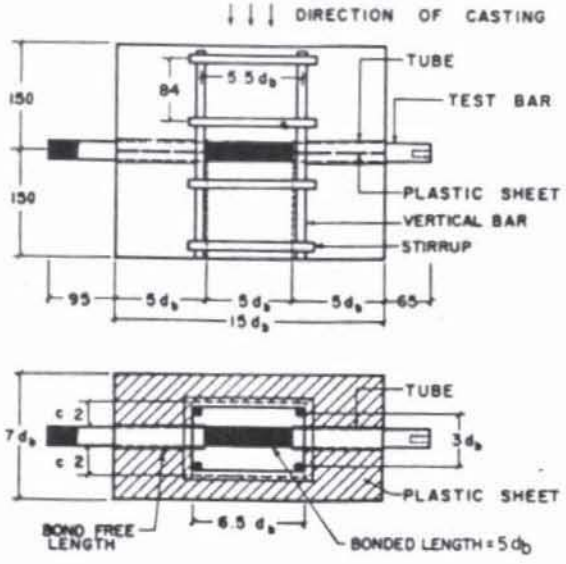

Fig. 1: Test specimen

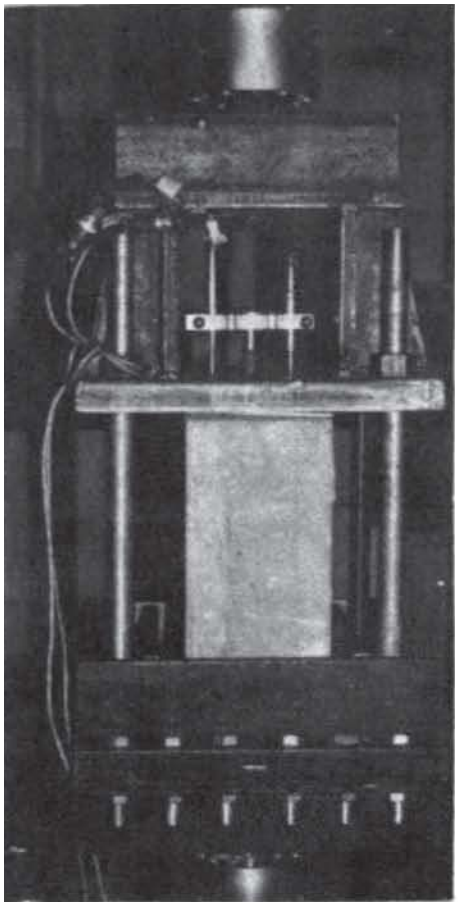

Fig. 2: Photo illustrating test set-up

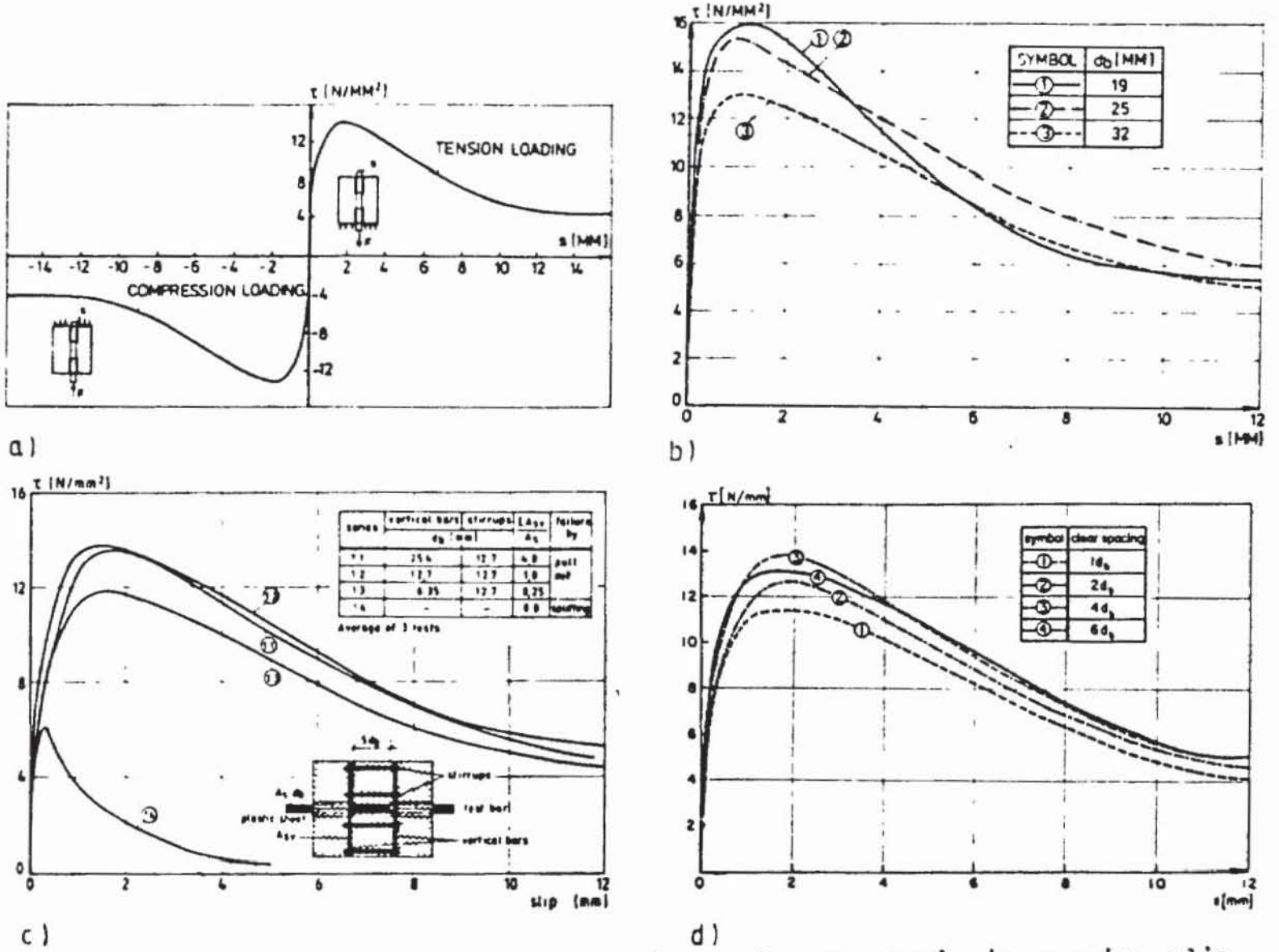

Fig. 3: Test results under monotonic increasing slip

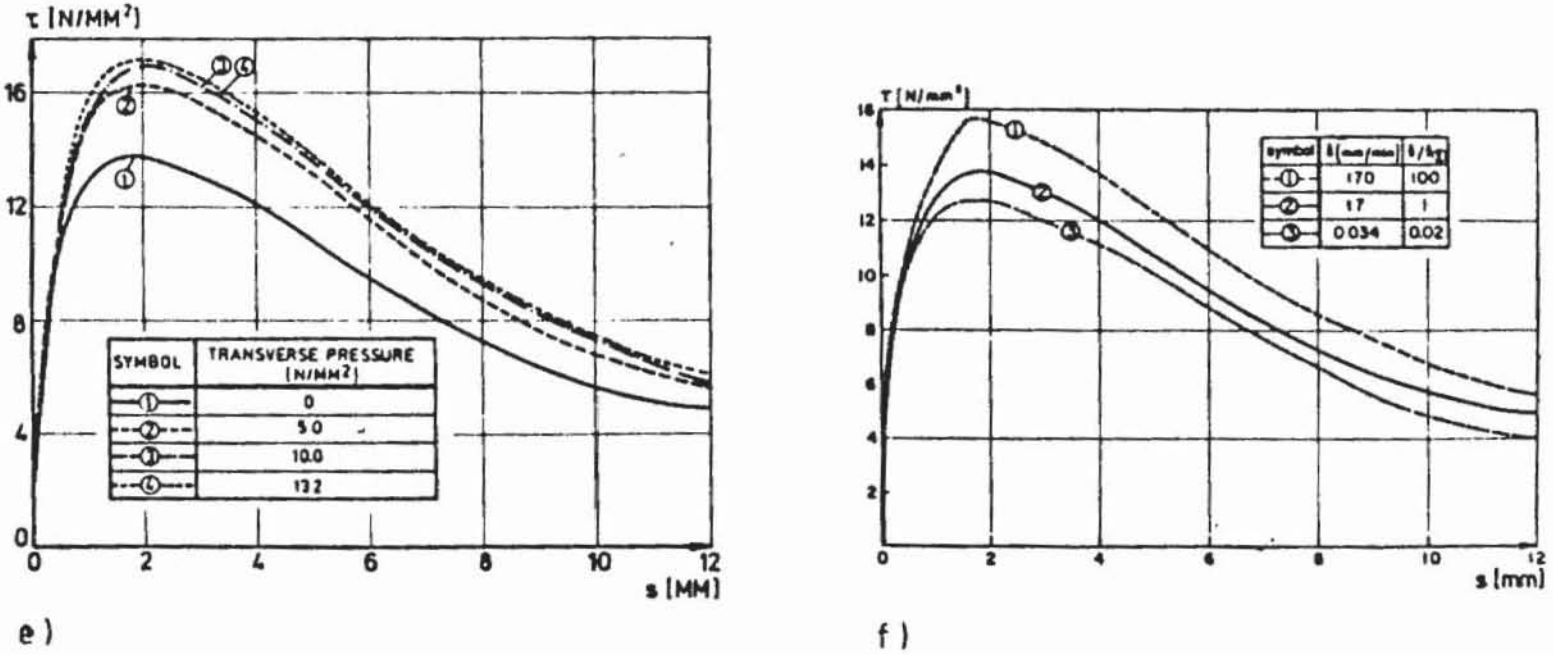

Fig. 3: Test results under monotonic increasing slip

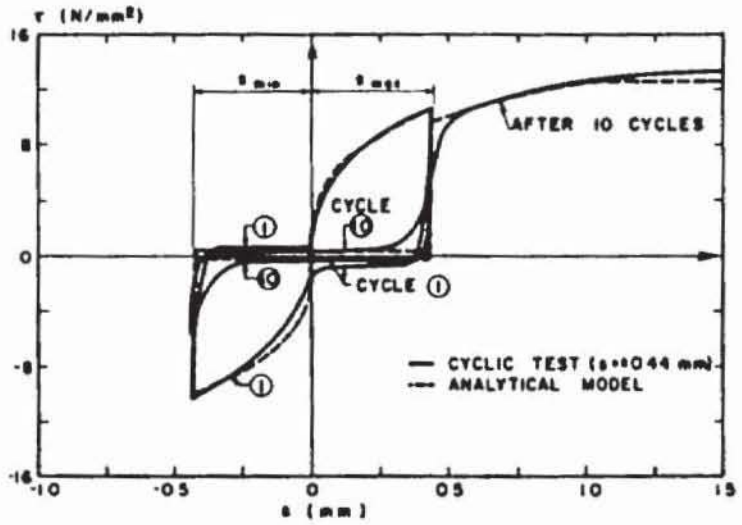

a) Cycling between s = ∓ 0,44 mm

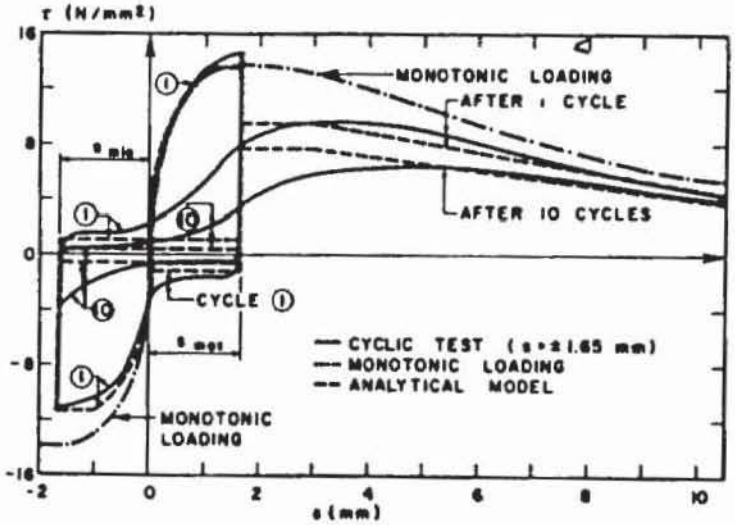

b) Cycling between s = ∓ 1,65 mm

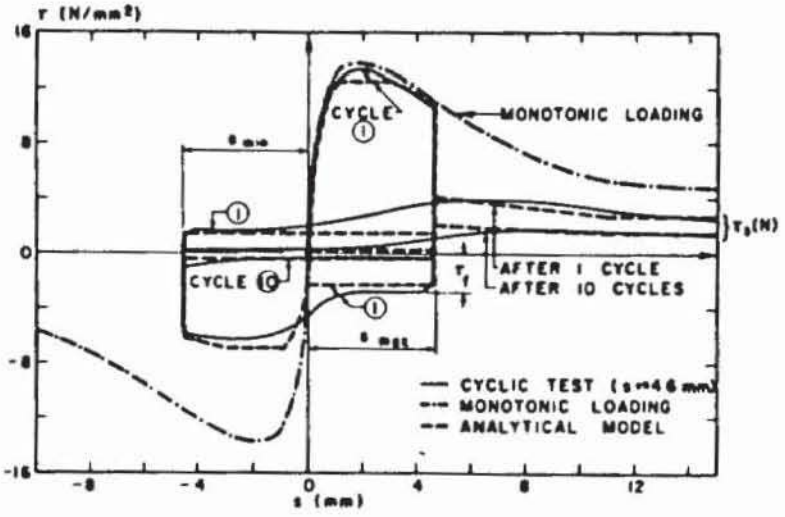

c) Cycling between s = ± 4,6 mm

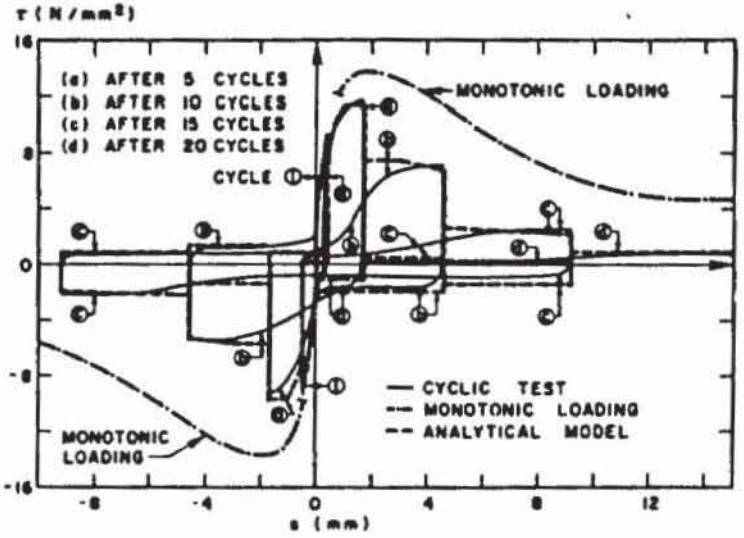

d) Cycling under different increasing s_{max}

Fig. 4: Comparison of experimental and analytical results on local bond stress-slip relationship

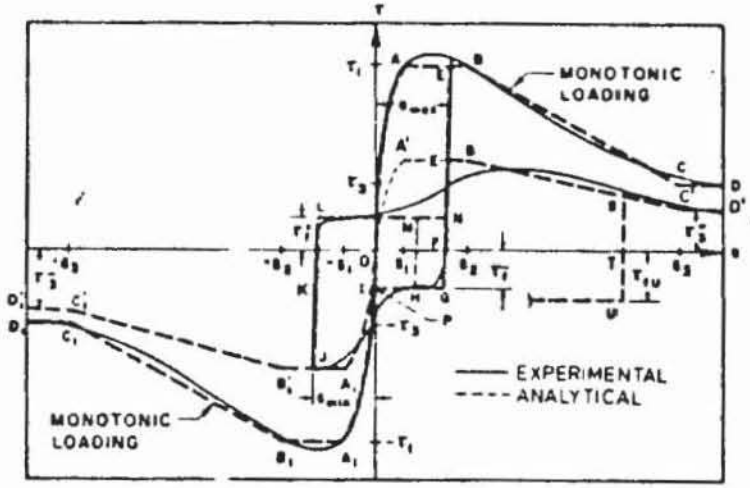

Fig. 5: Proposed analytical model for local bond stress-slip relationship

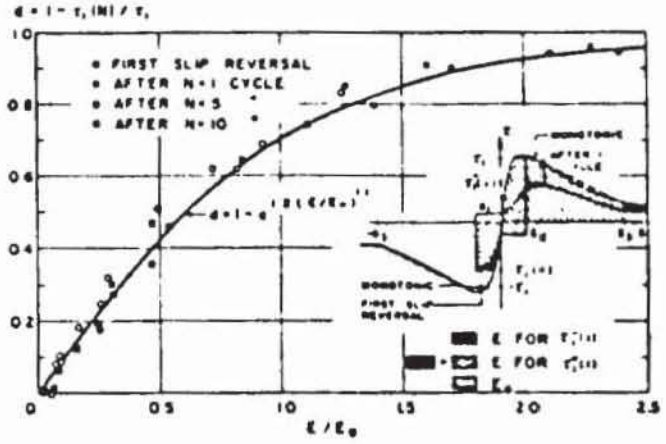

Fig. 6: Damage parameter d as a function of the dimensionless energy dissipation

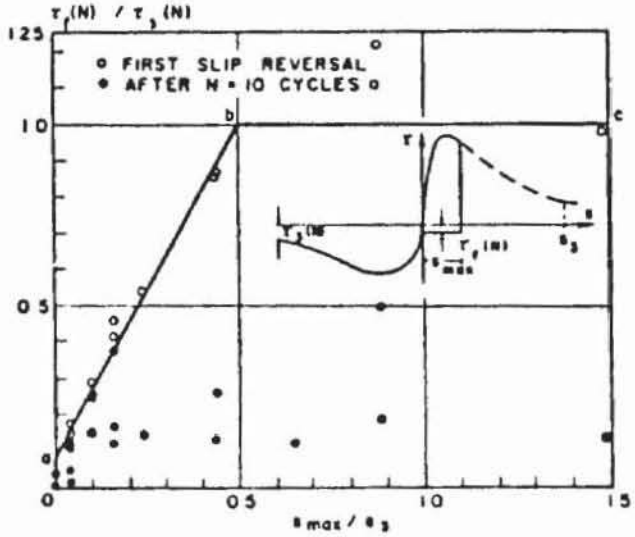

Fig. 7: Relationship between frictional bond resistance $_f(N)$ and the corresponding ultimate frictional bond resistance $_3(N)$

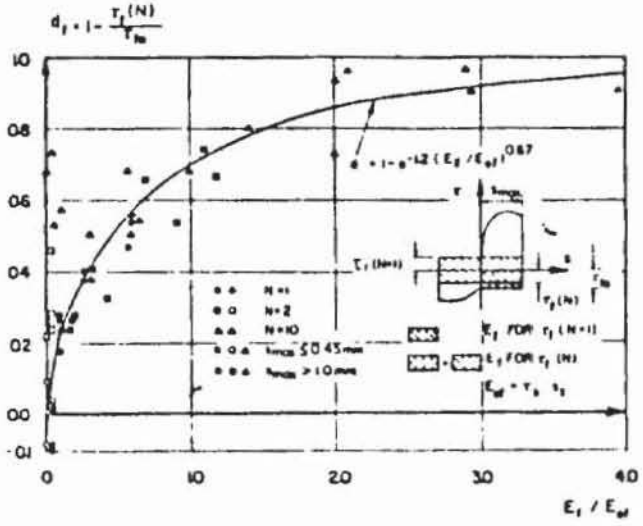

Fig. 8: Damage parameter d_f as a function of the dimensionless frictional energy dissipation

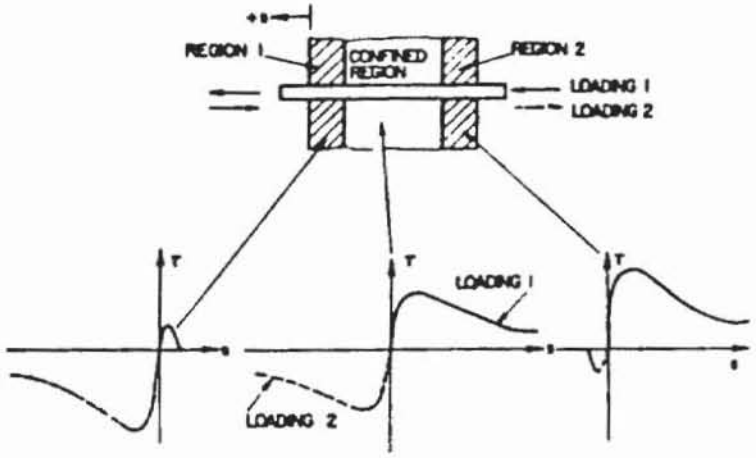

Fig. 9: Bond stress-slip relationships under monotonic loading for different regions in a joint

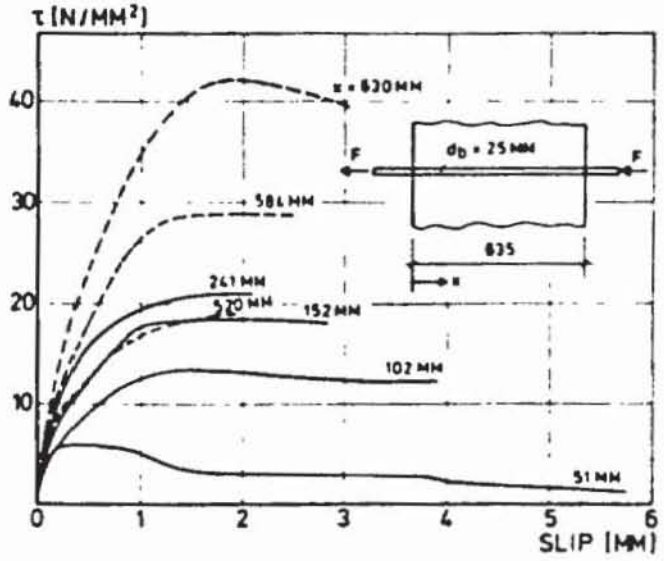

Fig. 10: Local bond stress-slip relationships for various points along the anchorage length, after /9/